Dynamic Simulation of Metal Transfer in GMAW — Part 2 : Short-Circuit Transfer Mode

The break-up mechanism of short-circuit transfer is analyzed dynamically to find out the effects of the welding parameters

BY S. K. CHOI, S. H. KO, C. D. YOO AND Y.-S. KIM

ABSTRACT. Short-circuit transfer is simulated dynamically by adopting the Volume of Fluid (VOF) method to analyze the effects of welding parameters on metal transfer. Appropriate initial and boundary conditions are imposed to simulate short-circuit transfer. The free surface profiles, pressure and velocity distributions are computed numerically during short-circuit transfer. The effects of the welding current, drop volume, contact area and wire feed rate on metal transfer are analyzed through variations of the pinch radius and break-up time. In the early stage of transfer, the molten metal in the bridge is transferred to the weld pool mainly due to the capillary pressure. The electromagnetic force becomes a dominant factor in the later stages of transfer. The effects of a current waveform on the characteristics of the metal transfer also are simulated.

Introduction

Short-circuit transfer occurs as the molten drop touches the weld pool surface in a low current range. Due to the low heat input, it has been used for thin-plate welding. The short-circuit mode is inherently unstable because of repetitive arc extinction and reignition. Because short-circuit transfer is a very complex phenomenon affected by various parameters, a theoretical model that includes all these factors has not been developed. Therefore, various experimental approaches have been widely utilized, especially the use of high-speed cameras. Analysis of the images indicates that spatter is generated mostly in the initial and final stages of the short-circuit transfer due to the high electromagnetic pinch force (Ref. 1). Based on this experimental observation, power supplies for spatter reduction have been developed to modulate the current levels in the initial and final stages of transfer (Refs. 2, 3).

Similar to other metal transfer modes in gas metal arc welding (GMAW), the short-circuit mode alsois affected by various welding parameters such as the welding current, voltage, wire feed rate and shielding gas composition (Ref. 4). While many experimental and theoretical studies have been carried out on the globular and spray transfer modes (Refs. 5, 6), only a few attempts have been made to model short-circuit transfer theoretically (Refs. 7, 8). Although it is widely accepted that the electromagnetic force plays an important role in the short-circuit mode, the relationship between the welding parameters and metal transfer has not been analyzed quantitatively.

In modeling of short-circuit transfer, Ishchenko (Ref. 7) predicted the velocity and acceleration of the molten bridge from the change in the surface tension energy. In his model, the effects of the welding current have not been included. Recently, Maruo (Ref. 8) utilized the Marker and Cell (MAC) method (Ref. 9) to simulate short-circuit transfer including the effects of surface tension, gravity and electromagnetic force. The free surface profile and fluid velocity within the molten bridge were computed numerically and the calculated results showed reasonably good agreement with the experimental data. However, magnetic flux density was used to impose the boundary conditions, which may not be suitable for the complex geometry of the molten bridge and weld pool.

In this work, the Volume of Fluid (VOF) method (Ref. 10) is adopted to simulate the short-circuit mode. The electromagnetic force is formulated and current density is used as the boundary condition instead of the magnetic flux density. The parameters of the current waveform to reduce spatter are suggested and their effects on metal transfer are simulated.

KEY WORDS

Dynamic Simulation
Short-Circuit Transfer
VOF Method
Free Surface Profile
Capillary Pressure
Electromagnetic Force

S. K. CHOI, S. H. KO and C. D. YOO are with the Dept. of Mechanical Engineering, KAIST, Taejon, Korea. Y.-S. KIM is with the Dept. of Material Science and Engineering, Hong Ik Univ., Seoul, Korea.

Formulation

The formulation of the VOF method was explained in a previous report for globular and spray transfer modes (Ref. 11). The relating equations are briefly explained here followed by the initial and boundary conditions for short-circuit transfer. Assuming the molten bridge and weld pool to be axi-symmetric and the material properties to be constant, the motion of an incompressible fluid is governed by the continuity and momentum equations and the equation relating to the function F:

$$\nabla \cdot v = 0 \tag{1}$$

$$\frac{\partial v}{\partial t} + (v \cdot \nabla)v = -\frac{1}{\rho}\nabla p + \upsilon \nabla^2 v + \frac{f}{\rho} \tag{2}$$

$$\frac{\partial F}{\partial t} + (v \cdot \nabla)F = 0 \tag{3}$$

where ρ, v and f denote the mass density, kinematic viscosity and body force vector, respectively. The body force includes the electromagnetic force, as well as gravity. The pressure on the free surface is determined by the surface tension and

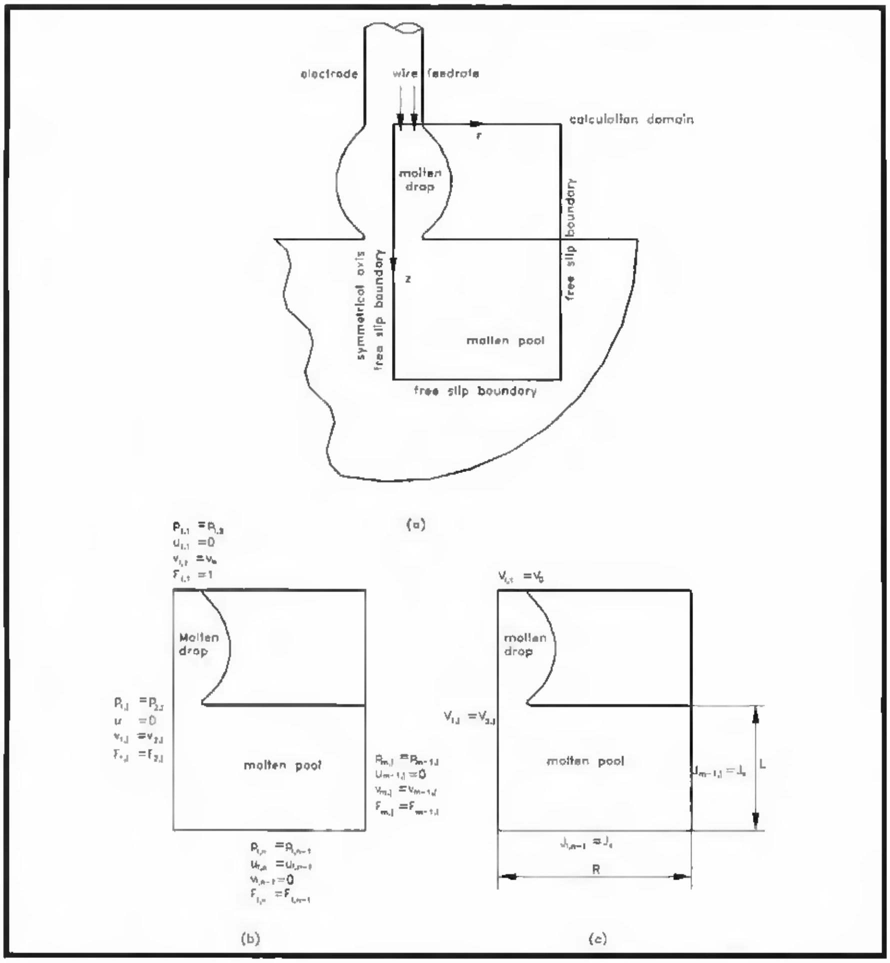

Fig. 1 — Initial and boundary conditions. A — Initial shape and solution domain; B — conditions for velocity and pressure; and C — conditions for voltage and current density.

radius of curvature.

The electromagnetic force generated by the welding current and self-induced magnetic field is expressed as

$$F_m = J \times B \quad (4)$$

where J represents the current density vector and B the magnetic flux density vector that is generated by the welding current in the z direction. Within the bridge and weld pool, the current density is calculated as the derivative of the voltage that satisfies the Laplace equation:

$$J = -\sigma \nabla V \quad (5)$$

$$\nabla^2 V = 0 \quad (6)$$

where σ is the electrical conductivity of the molten metal. For more information about the VOF method and formulation of the metal transfer in detail, refer to Hirt and Choi (Refs. 10, 11).

The initial and boundary conditions are imposed to simulate the short-circuit mode, as shown in Fig. 1. When the molten drop initially touches the weld pool surface, the pool surface is assumed to be flat and the initial molten drop is assumed to be spherical. Since thermal analysis is not included in this work, the weld pool is assumed to be cylindrical. A free-slip condition is enforced along the z axis, as well as on the boundary surface of the molten pool. The wire feed rate is given on the interface between the solid electrode and molten drop and the no-slip condition is imposed on this interface when there is no wire feed rate — Fig. 1A. The conditions for the velocity and pressure are illustrated in Fig. 1B, and those for the voltage and current density are shown in Fig. 1C.

When the pendant drop contacts the weld pool surface, the arc is extinguished and the entire welding current is conducted to the weld pool through the molten bridge. Therefore, no current flows through the free surface, which is expressed as

$$\sum_{\text{neighbor}} (J \cdot A) = 0 \quad (7)$$

where A denotes the area of the neighboring cell adjacent to the free surface cell. The above equation implies that the amount of the current input from the neighboring cells is equal to that of the current output to the neighboring cells within the fluid. Thus, there is no current conducted through the free surface.

Table 1 — Material Properties Used in This Work

Mass density, ρ	7860 (kg/m³)
Kinematic viscosity, ν	2.8×10^{-7} (m²/s)
Surface tension coefficient, γ	1.5 (N/m)
Electrical conductivity, σ	8.54×10^5 (ohm/m)
Permeability, μ	$4\pi \times 10^{-7}$ (H/m)

The current density on the boundary surface of the molten pool is assumed to be constant, and is derived as

$$J_o = I/(\pi R^2 + 2\pi RL) \quad (8)$$

where R and L are the radius and depth of the cylindrical weld pool, respectively — Fig. 1C. The above equations are converted into the corresponding difference forms for numerical computation. The numerical procedure of the VOF method for the short-circuit transfer is similar to that for the globular and spray modes (Ref. 11).

Results and Discussions

A 1.2-mm-diameter steel electrode was selected for simulation and the material properties are listed in Table 1. The dimensions of the solution domain are 4 and 6 mm in the r and z directions, respectively, and a square cell with 0.1 mm length is used.

Free Surface Profiles

The free surface profiles of the molten bridge and weld pool are calculated when the welding current and initial drop volume vary. The dynamic variation of the free surface profiles when the welding current is 0, 100 and 300 A is illustrated in Fig. 2. The initial conditions for this simulation are selected as the following: the molten drop volume is 10 mm³, contact radius 0.6 mm and wire feed rate 70 mm/s. When the current is not conducted (Fig. 2A), the gravity and capillary pressure due to the surface tension and curvature are the driving forces for the metal transfer. As will be explained later, the effect of gravity is negligible compared with that of the capillary pressure. Although no electromagnetic force is exerted, necking occurs at the contact surface due to the self-failure effect (Ref. 7). The free surface profile with 100 A is found to be similar to that without the current — Fig. 2B. It appears that the electromagnetic force does not affect the fluid motion significantly in the low current range. Therefore, the driving force in the early stage of the transfer should be the capillary pressure rather than the electromagnetic force. When the current is increased to 300 A (Fig. 2C), the break-up time becomes shorter. However, there is only a minor difference in the free surface profile compared with the results of the low current in the final stage of transfer. The weld pool surface becomes depressed near the break-up point, which agrees with the previous results (Ref. 8).

For the initial drop volumes of 5, 7.5 and 10 mm^3, corresponding free surface profiles are illustrated in Fig. 3. The welding current is 100 A and other conditions are the same as in Fig. 2. The break-up time increases for larger drops because the fluid volume to be transferred is increased. The bridge profile variations are similar in most cases and the breakup occurs consistently at the contact surface as in Fig. 2. From these results, it is clear that the break-up time depends on welding parameters such as the welding current and initial drop volume, but the free surface profile is not influenced significantly by these parameters. Although the simulation results are not compared with the experimental data, the general trends agree with the previous work (Ref. 8).

Pressure and Velocity Distributions

The calculated pressure distributions at 100 and 300 A are illustrated in Fig. 4. The initial and boundary conditions are the same as in Fig. 2. When the welding current is 100 A and the time lapsed after contact is 2 ms (Fig. 4A), the pressure within the bridge is mostly uniform. The low pressure near the contact region is generated due to the negative curvature. The contribution of the electromagnetic force is relatively small because of the low current density within the bridge. The maximum electromagnetic force in the bridge is 3.66×10^6 N/m^3. At a short-circuit time of 6 ms, which is just before breakup (Fig. 4B), the pressure increases noticeably at the necking region. This is caused by the decreased radius of curvature, as well as the increased current density, which results in an increase of the maximum electromagnetic force to 1.01×10^8 N/m^3. When the current is increased to 300 A (Fig.4C), the pressure increases significantly in the bridge and its distribution is also different from that of 100 A. The maximum electromagnetic force is 3.34×10^7 N/m^3. In the final stage of transfer (Fig. 4D), the maximum electromagnetic force is increased to 2.72×10^8 N/m^3.

The velocity distributions with 100 and 300 A are illustrated in Fig. 5. While

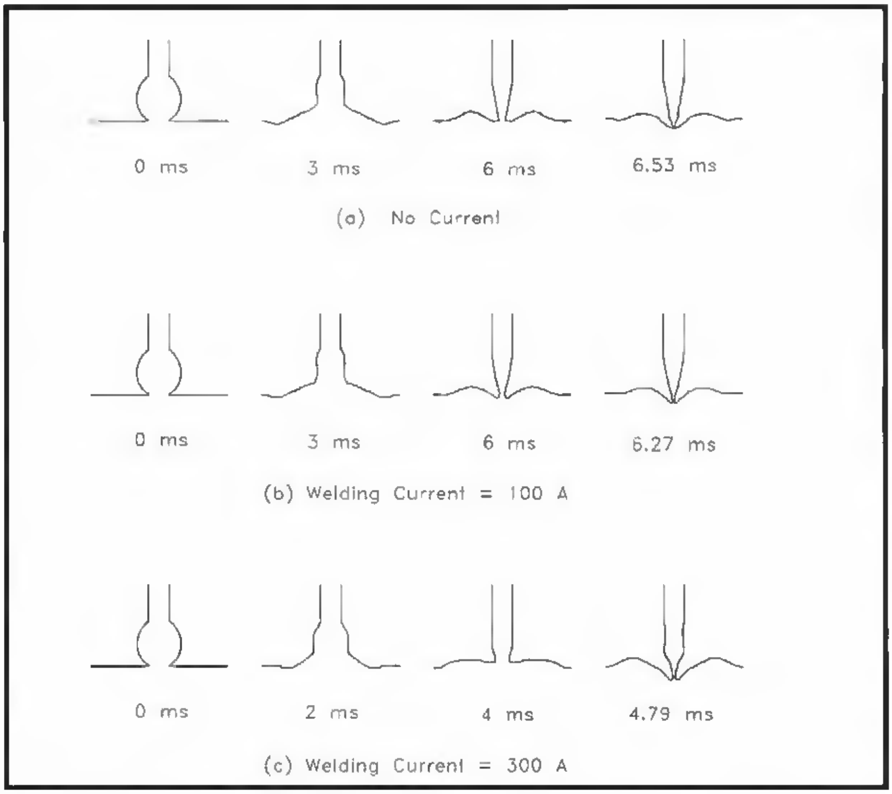

Fig. 2 — Bridge profiles for various currents with drop volumes of 10 mm^3. A — No current; B — 100 A; and C — 300 A.

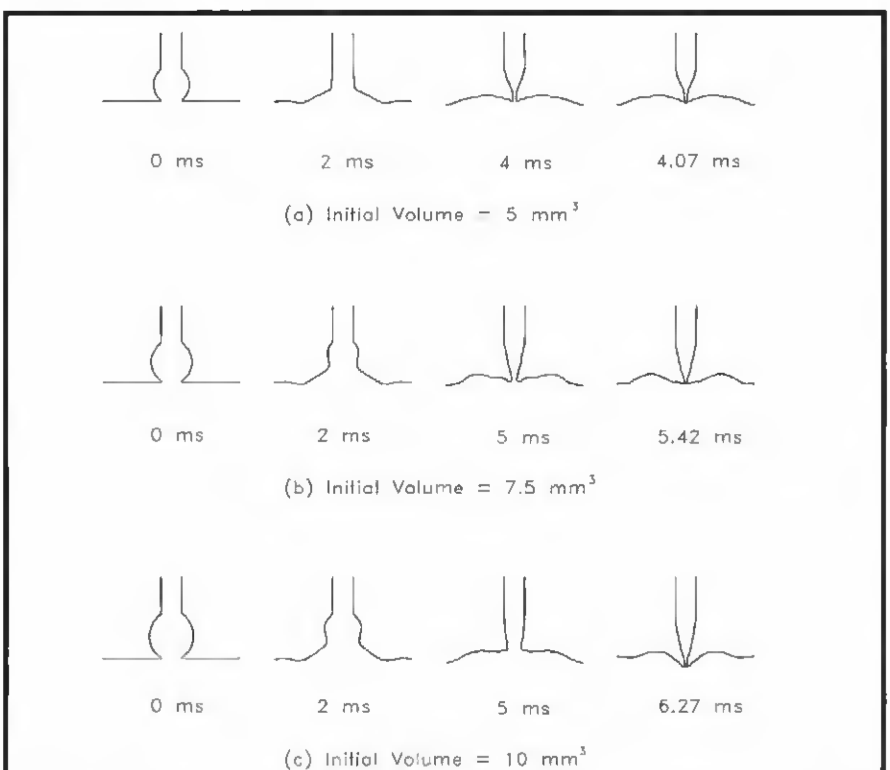

Fig. 3 — Bridge profiles for various drop volumes at 100 A. A — 5 mm^3; B — 7.5 mm^3; and C — 10 mm^3.

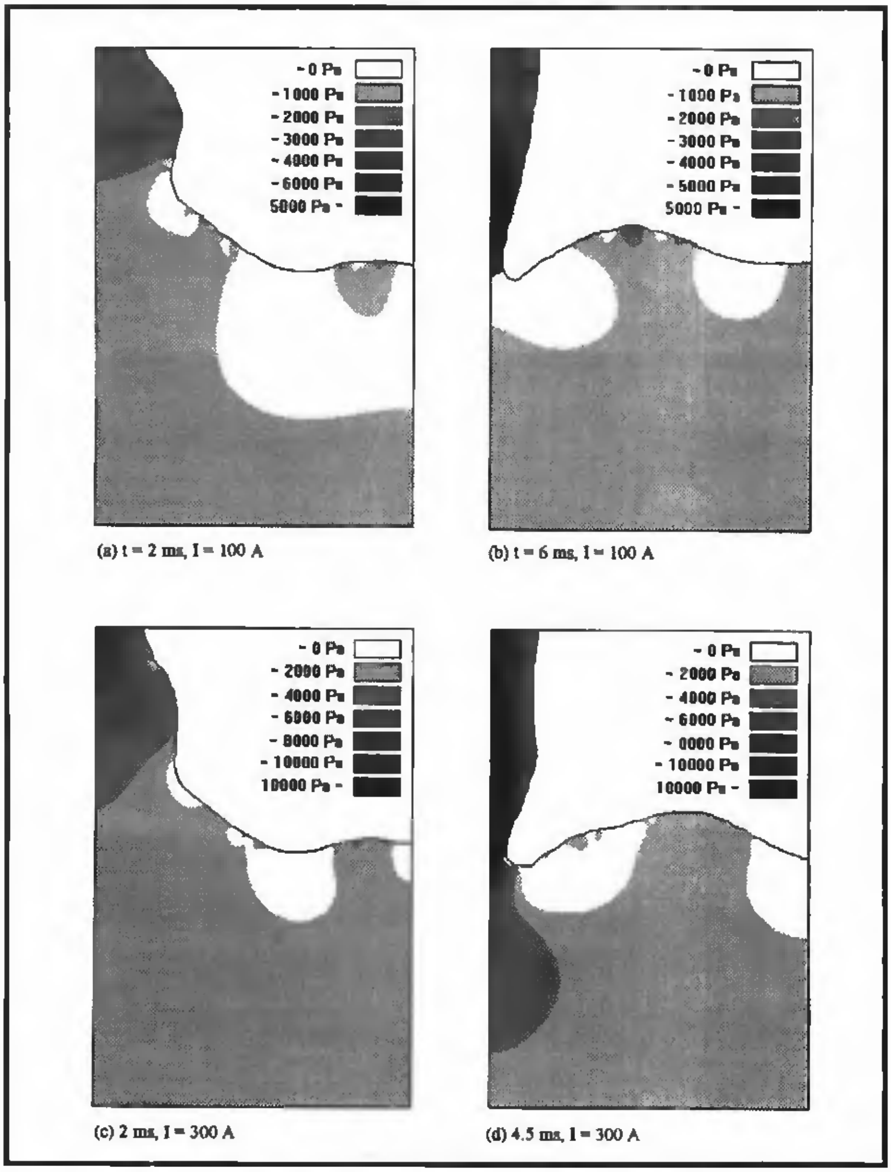

Fig. 4 — Pressure distributions at 100 and 300 A. A — t = 2 ms, I = 100 A; B — t = 6 ms, I = 100 A; C — t = 2 ms, I = 300 A; and D — t = 4.5 ms, I = 300 A.

the flow in the axial direction is dominant in the early stage of the transfer, a significant flow in the radial direction is calculated to exist in the bulged bridge and weld pool near the bridge — Fig. 5A, C. The maximum velocities in the bridge are 0.8 and 0.9 m/s for 100 and 300 A, respectively, and flow in the weld pool is not noticeable. In the final stage of transfer (Fig. 5B, D), the velocity increases and the axial flow becomes predominant in the bridge. The maximum velocities increase to 2.4 and 2.9 m/s for 100 and 300 A, respectively. Weld pool convection at this stage is developed in a counterclockwise direction and the pool surface becomes convex due to this convection.

Effects of Welding Parameters on Metal Transfer

Based on previous works (Refs. 7, 8), in addition to the welding current and initial drop volume, the contact area and wire feed rate are the welding parameters affecting metal transfer. The effects of these parameters are analyzed through the variations in the break-up time and pinch radius. The pinch radius is defined as the minimum radius of the bridge.

The effects of the welding current up to 300 A on the short-circuit transfer are shown in Fig. 6. The initial drop volume is 10 mm^3, contact radius 6 mm and wire feed rate 70 mm/s. The pinch radius increases to the maximum value in the initial stage of transfer and then decreases in later stages. In general, it takes about 1.2 ms to reach the maximum pinch radius, which is approximately 1 mm. When the current is not conducted, only gravity and surface tension are exerted. Although it is not included in the plot, there is almost no difference in the pinch radius variations with or without gravity, which implies

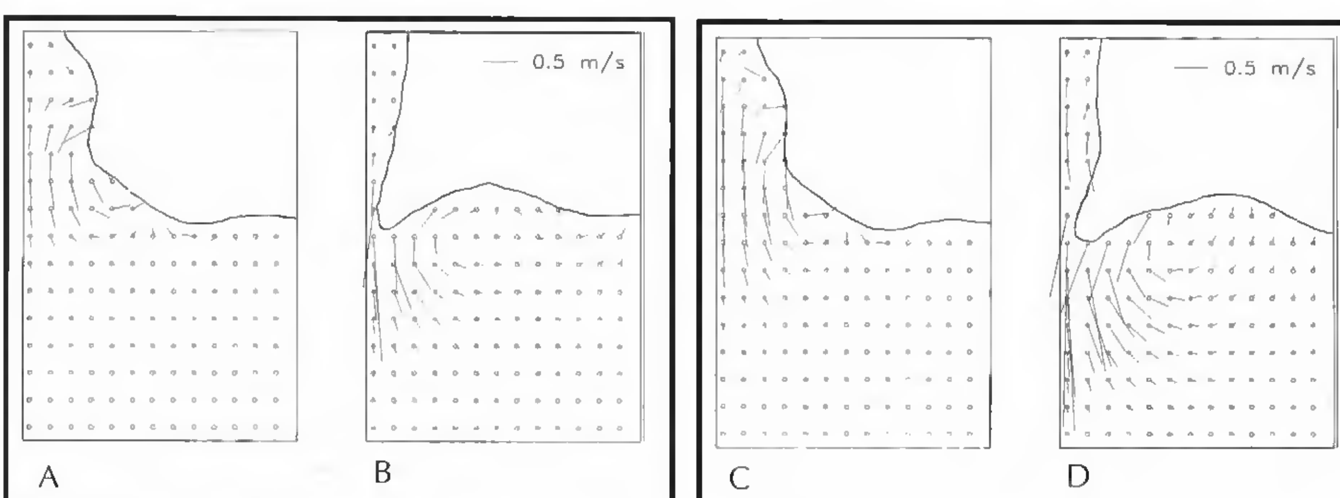

Fig. 5 — Velocity distributions at 100 and 300 A. A — t = 2 ms, I = 100 A; B — t = 6 ms, I = 100 A; C — t = 2 ms, I = 300 A, and D — t = 4.5 ms, I = 300 A.

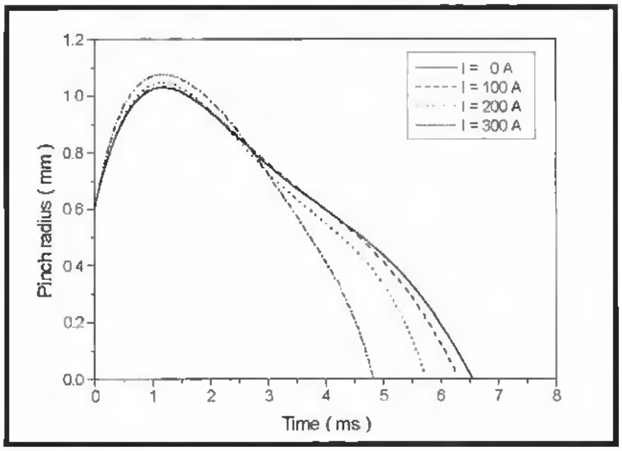

Fig. 6 — Effects of welding current on pinch radius and break-up time.

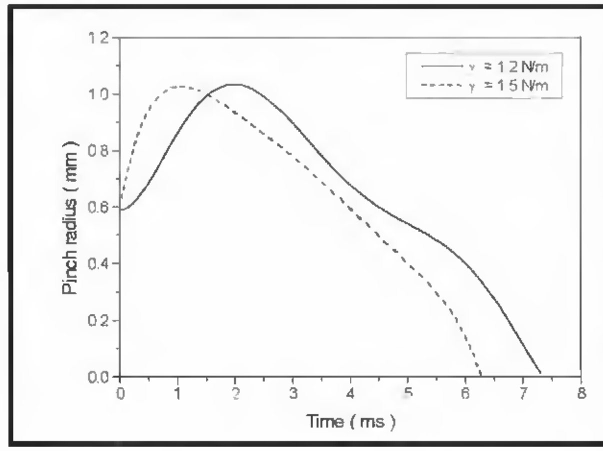

Fig. 7 — Effects of surface tension on pinch radius and break-up time.

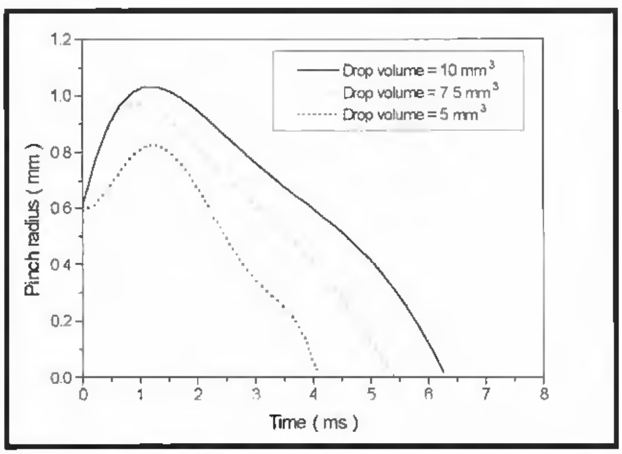

Fig. 8 — Effects of initial drop volume on pinch radius and break-up time.

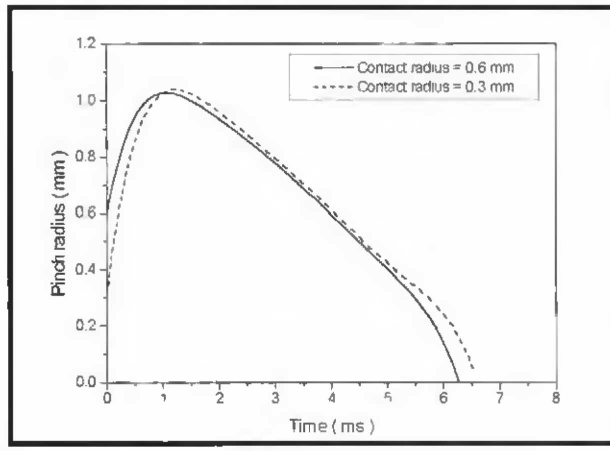

Fig. 9 — Effects of initial contact radius on pinch radius and break-up time.

that the effects of gravity on the metal transfer are negligible. This is known from the Bond number, which becomes less than 0.1 ($Bo = \rho g d^2/\gamma$). The variations in the pinch radius with no current conduction and at 100 A are also found to be very similar. As mentioned earlier, it is clear that the electromagnetic force does not have significant effects on metal transfer in the low current range and the metal transfer is dominated by the capillary pressure. When the welding current is increased to 200 A, the effects of the current become noticeable in the later stage of the transfer. When the current is increased to 300 A, the maximum pinch radius becomes slightly larger than with lower currents. After reaching the maximum pinch radius, the pinch radius decreases faster and the break-up time is reduced significantly. It is thus evident that the electromagnetic force becomes a dominant factor in the later stage of transfer.

Since the capillary pressure plays an important role in the early stage of transfer, the effects of the surface tension are simulated as illustrated in Fig. 7. With a lower surface tension of 1.2 N/m, the break-up time increases compared with the case of 1.5 N/m. While the maximum pinch radii are almost the same for both cases, it takes about 1.2 and 2.2 ms to reach the maximum pinch radius for surface tensions of 1.5 and 1.2 N/m, respectively. The reason for the time difference is that lower surface tension generates lower capillary pressure for the same curvature in the early stages of transfer. After reaching the maximum pinch radius, the pinch radius decreases approximately at the same rate so that the resultant break-up time increases by 1 ms for the case of 1.2 N/m. It thus seems that the break-up time is affected by the time to reach the maximum pinch radius.

The effects of the initial drop volume on the pinch radius are illustrated in Fig. 8, where the welding current is fixed at 100 A, and other conditions are the same as Fig. 6. The initial drop volumes are selected to be 5, 7.5 and 10 mm^3 for this simulation. With the smaller drop volume, the maximum pinch radius becomes smaller because of the limited volume of the fluid to form a bridge. The time to reach the maximum pinch radius is less than 1.5 ms in general. As there is not much difference in the rate change of the pinch radius after reaching the maximum values, the break-up time depends on the maximum pinch radius: the larger the maximum pinch radius, the longer the break-up time. Considering the fact that the welding current has little effect on metal transfer in the early stages, the initial drop volume should be an important factor in determining the break-up time.

The effects of the contact radius on metal transfer are illustrated in Fig. 9, where the contact radius is selected to be 0.3 and 0.6 mm and other conditions are the same as Fig. 6. In both cases, the max-

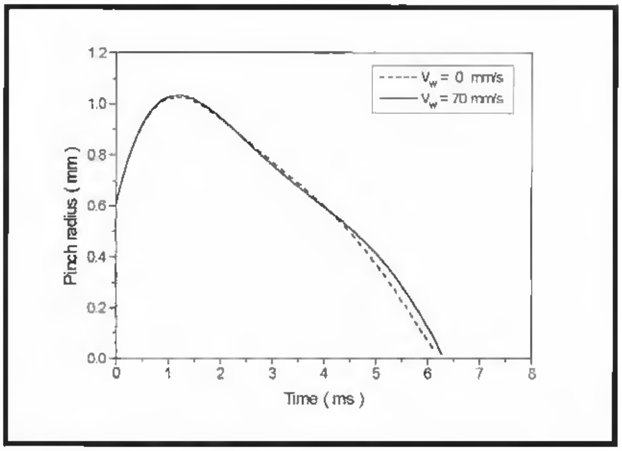

Fig. 10 — Effects of wire feed rate on pinch radius and break-up time.

imum pinch radii are almost the same and the break-up time increases slightly with a smaller contact radius. The results show that the initial contact radius has a less significant effect on metal transfer compared with the welding current and initial drop volume.

The effect of wire feed rate is illustrated in Fig. 10. There is little difference in the pinch radius between the cases with no wire feed and with a wire feed rate of 70 mm/s. This phenomenon can be explained by considering the fluid velocity in the bridge and the wire feed speed. According to the previous calculation (Fig. 5A, B), the maximum fluid velocities in the bridge are between 0.8 and 2.5 m/s, which are much faster than the wire feed speed. Therefore, the contribution of the wire feed speed on fluid flow and drop volume is very small and overall effects of the wire feed rate on the metal transfer should be negligible.

Effects of Current Pulse on Metal Transfer

As mentioned earlier, spatter is generated mainly in the initial and final stages of transfer. Therefore, significant efforts have been directed to devise current waveforms for spatter reduction. General principles in determining the current waveform are suggested based on the simulation results.

When the molten drop touches the weld pool surface, the arc is extinguished and the welding current should increase abruptly due to the decreased resistance. The electromagnetic force increases significantly. If the symmetry of the bridge is disturbed, spatter can be generated due to the unbalance of the large electromagnetic force. The size of spatter occurring in this stage tends to be large because the entire drop is repelled. Considering that the molten bridge without current conduction does not generate spatter (for example, the soldering process), spatter generation in the initial stage can be decreased by lowering the current level just before the short-circuit. Because the current does not affect metal transfer significantly in the early stage as in Fig. 6, the current should he kept low, but high enough to maintain the bridge and weld pool in the molten state by joule heating. As it takes less than 1.5 ms to reach the maximum pinch radius in most cases, it is suggested that the low current level be maintained until 1.5 ms after the short-circuit. It is noted that the high current would increase the length of the bridge, and may lead to a kink instability.

Once the maximum pinch radius is reached, the current should be increased to promote metal transfer. As the pinch radius becomes smaller in the final stages of transfer, the current density and electromagnetic force increase, which results in spatter generation similar to the initial stage of transfer. The size of the spatter should be smaller than that of the initial stage because the volume of the bridge is small. As the effects of the welding current become noticeable after approximately 3 ms for the case of 300 A (Fig. 6), it is suggested that the current then be lowered. Again, the reduced current level should be high enough to maintain the bridge and weld pool in the molten state as an early stage of transfer.

A current pulse was designed based on the above propositions and a simulation was carried out — Fig. 11. The

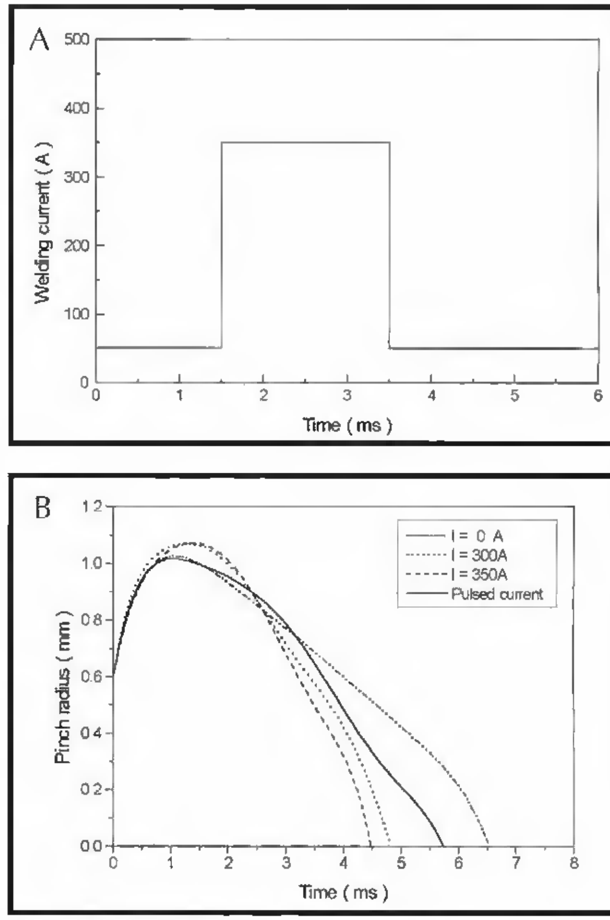

Fig. 11 — Results of pulsed current for spatter reduction. A — Pulsed current waveform; B — comparison between pulsed and constant currents.

modified current waveform is similar to pulsed current — Fig. 11A. Because thermal factors are not included in this work, the magnitude of the peak and base currents is selected based on data by others (Refs. 2, 3). The base current is maintained at 50 A until 1.5 ms and after 3.5 ms and the peak current is 350 A. The calculated results with constant current at 0, 300 and 350 A are also plotted for comparison — Fig. 11B. The maximum pinch radius of the pulsed current becomes smaller and the pinch radius decreases more gradually than with 300 and 350 A. The break-up time of the pulsed current is longer than that of 300 and 350 A, but is shorter than that with no current. Thus, proper design of the current waveform would decrease the break-up time with little spatter generation.

It is noted that the temperature variation in the bridge should be taken into account for better understanding of spatter generation. When the temperature of the necking region approaches the vaporizing temperature of the molten metal due to joule heating, the bridge may explode instead of breaking in a stable manner.

The current reduction in the final stage is effective in lowering the temperature as well as the electromagnetic force in the bridge. The amount of spatter can be reduced by stabilizing the metal transfer and preventing possible explosion. Therefore, a further investigation including thermal analysis should be incorporated in the present VOF algorithm for thorough understanding of short-circuit transfer.

Conclusions

Short-circuit transfer is simulated using the VOF method, and the results lead to the following conclusions:

1) The capillary pressure is the dominant factor affecting short-circuit transfer in the early stages and the electromagnetic force due to the welding current becomes more important in the later stages. Breakup of the bridge is promoted with higher surface tension due to higher capillary pressure and the effect of gravity on metal transfer is negligible.

2) The welding current and initial drop volume affect the rate change of the pinch radius and maximum pinch radius that determines the break-up time. Therefore, the welding current and drop volume are the most important parameters in determining the dynamics of transfer. The initial contact radius and wire feed rate have less significant effects on metal transfer.

3) To reduce spatter, it is suggested that the welding current be reduced before 1.5 ms and after 3.5 ms so that stable metal transfer can be achieved by reducing the electromagnetic force as well as the temperature in the bridge.

Acknowledgments

The authors wish to express their sincere appreciation to Prof. J. M. Hyun at KAIST and Prof. T. W. Eagar at MIT for their invaluable advice and comments. This work is partially funded by the MTIE in Korea.

References

1. Lipei, J., Jingchang, L., and Zhihuan, W. 1987. The effect of the dynamic behavior of welding rectifiers on spatter. *Welding International* 1(3): 129–133.

2. Yamamoto, H., Harada, S., and Yasuda, H. 1990. The development of welding current control system for spatter reduction. *Welding International* 4(5): 398–407.

3. Stava, E. K. 1993. The surface-tension-transfer power source: A new, low-spatter arc welding machine. *Welding Journal* 72(1): 25–29.

4. Lancaster, J. F. 1985. *The Physics of Welding*, 2nd Ed., Pergamon Press.

5. Kim, Y.-S., and Eagar, T. W. 1993. Analysis of metal transfer in gas metal arc welding. *Welding Journal* 72(7): 169-s to 178-s.

6. Rhee, S., and Kannatey-Ashibu, E. Jr. 1992. Observation of metal transfer during gas metal arc welding. *Welding Journal* 71(10): 381-s to 386-s.

7. Ishchenko, Y. S. 1993. Relationships governing droplet transfer during a short-circuit. *Welding International* 7(8): 627–631.

8. Maruo, H., Hirata, Y., and Goto, N. 1992. Bridging transfer phenomena of conductive pendent drop: The effects of electromagnetic pinch force on the bridging transfer. *Quarterly J. of JWS* 10(2): 251–258, (in Japanese).

9. Harlow, F. H., and Welch, J. E. 1965. Numerical calculation of time dependent viscous incompressible flow of fluid with free surface. *Phys. Fluids* 8(12): 2182–2189.

10. Hirt, C. W., and Nichols, B. D. 1981. Volume of fluid (VOF) method for the dynamics of free boundaries. *J. Comp. Phys.* 39: 201–225.

11. Choi, S. K., Yoo, C. D., and Kim, Y.-S. Dynamic simulation of metal transfer in GMAW, — Part 1: globular and spray transfer modes. *Welding Journal* 77(1): 38-s to 44-s.